05,12

Cobalt and nickel nanowires: dependence of structure and magnetic properties on conditions of production and ion irradiation

© D.L. Zagorskiy[1], R.A. Makarin[2,4], N.S. Perov[2], K.V. Shalomov[3], I.M. Doludenko[1], V.V. Ovchinnikov[3], N.V. Gushchina[3], D.V. Panov[1]

[1] National Research Center „Kurchatov Institute“, Moscow, Russia
[2] Moscow State University, Moscow, Russia
[3] Institute of Electrophysics, Ural Branch, Russian Academy of Sciences, Yekaterinburg, Russia
[4] MIREA — Russian Technological University, Moscow, Russia

E-mail: dzagorskiy@gmail.com

Received March 6, 2025
Revised March 6, 2025
Accepted May 5, 2025

Arrays of nanowires (NWs) with a diameter of 100 nm from Ni and Co have been obtained by matrix synthesis. Nickel samples were obtained at different temperatures of the electrolyte solution, and cobalt samples were obtained at different pH values. The magnetic properties were investigated by vibrational magnetometry. A multiple increase in saturation magnetization and coercive force was found for Ni-NWs with an increase in the electrodeposition temperature from 20 to 60 °C. A change in the pH of the cobalt electrolyte from 3 to 5 leads to a change in the NW structure, respectively, from cubic to hexagonal, with a noticeable change in magnetic parameters. The NW arrays were irradiated with argon ions with an energy of 15 keV with fluences from $8.6 \cdot 10^{11}$ to $6.3 \cdot 10^{15}$ cm^{-2}. When Co-NWs (with a hexagonal lattice type) are irradiated, a non-monotonic change in the hysteresis parameters is observed — an increase and subsequent decrease in saturation magnetization and a change in coercive force. In samples based on the other two types of NW, the effect of irradiation is ambiguous. Irradiation leads to a strong change in the shape of the tips of Co-NWs.

Keywords: matrix synthesis, metallic nanowires, ion irradiation, radiation damage, electron microscopy, X-ray phase analysis, saturation magnetization, coercive force.

DOI: 10.61011/PSS.2025.07.61891.32HH-25

1. Introduction

Nanowires (NW) are conventionally unidimensional nanomaterials that are of significant interest both from the fundamental science point of view (quantum-size properties), and when it comes to practical application (elements of microelectronics, spintronics devices, sensors) [1–3].

The popular method of their production is matrix synthesis — pores of the special growth matrices (templates) are filled with the required material. The matrix is most often either a porous aluminum oxide (PAO) [4] or a track membrane [5,6]. As a rule, the pores are filled with metals by galvanic (electrochemical) deposition [7]. The advantage of the matrix synthesis is its variability [8]. The features of NWs obtained by this method are their small (nanoscale) diameter, high aspect ratio, huge number of individual identical NWs in a conglomerate (array).

In its turn, making NWs from the iron group metal makes it possible to obtain magnetic materials of new types. In this case the controlled change of the shape and size (structures with high aspect ratio), and the production method are the additional effective methods to change the magnetic properties [9,10].

This paper studied the homogeneous single-component nanomaterials — NWs from cobalt or nickel. Note that historically the study of the magnetic NWs started exactly from the study of these simplest samples. And even though today the primary attention is paid to synthesis and study of the properties of more complex objects (NWs from alloys, laminar NWs and more complex structures), the interest in single-component NWs still remains. The study of NWs from iron, cobalt and nickel started in the end of the 20th century already. Comparative features of the synthesis of such NWs and their magnetic properties are described in papers [11,12], and the review of wide possibilities for their use is given in [13]. The features of making the NWs from these three metals are described in [14]. Some parameters of NWs from three basic ferromagnetic materials Fe, Co, Ni, and also the description of creating large gradient fields in such NWs are given in [15].

Some papers are dedicated to cobalt NWs. Thus, in [16] the features of Co-NW synthesis were studied in the pores of the polymer polycarbonate membrane using

pulse deposition. In paper [17] it is shown that Co-NWs grown in PAO by the method of pulse deposition from electrolyte with pH = 5, have hexagonal structure; also the strong dependence is shown between the structure and the magnetic properties and the diameter. In paper [18] Co-NWs are obtained in the pores of the membrane from polycarbonate; a rather acidic electrolyte was used; the process was carried out under direct voltage. NWs had a face-centered cubic (FCC) structure and were noticeably textured. In paper [19] Co-NWs were grown in PAO pores using alternating current. Authors [20] studied cobalt NWs grown under different conditions. Both papers showed that the NW structure depends on pH of the electrolyte.

Nickel NWs in [21–23] were produced in the PAO matrix. In [21] the authors describe the advantages of the pulse electric deposition. In paper [22] the hysteresis loops were measured for the obtained NW samples at different temperatures, the temperature dependence was determined for the main magnetic characteristics. In paper [23] the electroconductivity and isothermal magnetization were studied for NWs obtained by the method of pulse deposition. In [24] for electric deposition a polymer polycarbonate matrix was used: the proposed two-step method was applied to obtain hollow tubes with the controlled wall thickness.

The given examples show that the characteristics of the studied single-component NWs depend on the production conditions and are determined by many factors. This paper studies the impact of the electrolyte solution acidity at the structure and properties of Co-NWs, and also of the growth temperature on the properties of Ni-NWs.

The important factor that may impact the material properties is the radiation exposure. Recently methods have become popular that use the bundles of accelerated ions for the targeted modification of the material properties [25]. Besides, it is relevant to use the ion irradiation to evaluate the radiation stability of materials in the imitation experiments [26,27]. The simplest arrangement of material exposure to ions consists in the fact that when bombarded with high energy particles, partially the energy of these particles is transferred, causing the displacement of the crystalline lattice atoms that causes the formation of the defects of various types. When heavy ions are used with energies from several dozens to several hundreds of keV, in most cases dense cascades of atomic displacements are formed. In process of irradiation and at subsequent stages it is both possible to accumulate such defects and to partially annihilate the radiation defects. The latter may be happening, for example, at the grain boundaries or other structural heterogeneities. All these processes may provide for different effects, sometimes called radiation-induced. The reviews of the current state of the question on the impact of the irradiation on the crystals and metal materials are given in certain papers, for example, in the book [28].

It may be assumed that in case of unidimensional nanostructures the effect of the radiation exposure has certain specificity. However, by this time only some attempts have been made to study the effect in NWs. Thus, in the book [28], dedicated to the radiation exposure of nanostructures of various types, it is noted, in particular, that in such materials the role of the surface and the surface energy is high. Accordingly, these materials are characterized by the excess of the free energy and are rather non-equilibrium. This circumstance may cause specific evolution of the nanostructure exposed to radiation and cause changes in the characteristic properties. In paper [29] several options are proposed for the nanomaterial behavior when irradiated. The presence of a considerable number of interface surfaces (high share of the surface) contributes to the drain (removal) of arising radiation-induced defects. Radiation-induced defects will contribute to the annihilation of nanostructured nature, for example, to the transition into amorphous state. Irradiation may also cause recrystallization.

The NWs irradiation effect was studied in some experimental papers. In [30] the ion-beam modification of nickel and cobalt NWs with chlorine ions having energy of 3 MeV is described. The microscopy methods found some changes in the morphology of the surface and reduction of the oxide layer on the NW surface. In paper [31] the silver NWs were irradiated with helium ions with energy of 5 MeV. Upon achievement of certain threshold value (fluence $10^{16}\,cm^{-2}$), the crystalline structure was converted into the amorphous one. The authors [32] irradiated similar NWs from silver with protons having energy of 3 MeV and showed that already at fluence $10^{14}\,cm^{-2}$ NWs „were fused“ with each other to form a chain of NWs. When silver NWs were irradiated with carbon ions having energy of 5 MeV at fluence $10^{16}\,cm^{-2}$ in paper [33], first the sample electroconductivity increased (due to the formation of contacts between wires), and then the electroconductivity decreased (due to the increase in the defect degree in the NW).

In paper [34] we studied the impact of heavy ions Ar^+ and Xe^+ with energy of 20 keV at NWs from nickel and nickel alloy. Changes were found in the NW topography — bends and areas of melting; their nature depends on the fluence of ions and is explained by so called „area of thermal spikes“ — by nanoscale areas of burst energy release being the thermalized areas for passing of dense cascades of atomic displacements heated to several thousand degrees. In paper [35] the effect was studied from the bundle of ions C^+ and H^+ with considerably higher energy, 250 keV, on the nickel alloy; but in this case the main role in the NW changes was played by thermal spikes.

There are several papers that used ion irradiation to modify the magnetic properties of nanostructures. Thus, in papers [36–38] the impact is shown from the irradiation with ions He^+ on the type of anisotropy in multilayer ultrafine films Co—Pt and Co—Pd, which made it possible to observe the topological effect of Hall in the magnetic skyrmions [39]. In papers [40,41] the possibility is shown to use the implantation of ions He^+ in thin films Ta—CoFeB—MgO and Co—Pt for modification of

the surface interaction of Dzyaloshinsky–Moriya. In article [42] the formation of nanostructures being ferromagnetic inclusions in the paramagnetic, but well magnetized matrix in the thin films of $Fe_{0.6}Al_{0.4}$ alloy under exposure to irradiation with xenon ions having energy of 160 MeV was studied. However, the listed papers did not consider the unidimensional structures — nanowires.

To sum up, it may be noted that there are not too many papers on the effects of NWs exposure to radiation, they used different types of irradiation, and they are dedicated to various effects, which manifest themselves upon irradiation, therefore it is rather complicated to compare the obtained results. And there are practically no papers on the impact of irradiation on the magnetic characteristics of NWs. Therefore, the objective of the second part of this article was to study the radiation exposure (irradiation with heavy ions of low energy was used) at the obtained NWs of three types and detection of the change in their magnetic characteristics.

Note that in case of NW the interest in radiation-induced effects is first of all caused by the need to research the radiation stability of the produced material. Besides, the possibility of radiation modification is also studied: the effect of the directed change of the properties under various types of irradiation is known for the films and volume materials [25,28]. It may be assumed that it is also possible to select irradiation for NWs, which will result in the change of the operating parameters in the needed direction, for example, in the increase of the coercive force.

2. Experimental procedure

2.1. Materials and instruments

The growth (template) matrices used for synthesis of samples were the polymer track membranes (nuclear filters) produced by the Joint Institute for Nuclear Research (Dubna), with thickness of 12 μm, with pore diameter of 100 nm and surface density of the order of 10^9 cm^{-2}. The matrices were prepared by pre-treatment of their surface and development of a thin (with thickness of 1–2 μm) current-conducting copper layer on one side. The layer was developed by two-stage metallization: by thermal sputtering of copper in vacuum with subsequent galvanic „regrowth“ (also with copper) to the required thickness.

The obtained porous matrices with the metallized surface were then used as a matrix (template) to produce NWs by „charging“ the required metal into the pores by electric deposition method. For this purpose the membrane was placed into a galvanic cell, and the applied metal layer was a cathode. The process was carried out using a two-electrode arrangement; when nickel or cobalt were deposited, nickel or cobalt anodes were used, accordingly.

To synthesize Ni-NW, a solution with composition of $NiSO_4 \cdot H_2O$ — 200 g/l; $NiCl_2$ — 30 g/l; H_3BO_3 — 25 g/l; sodium lauryl-sulphate — 1 g/l (so called Watt's plating solution) was used. The process was carried out under the direct voltage of 1.5 V. Synthesis of Ni-NW was carried out at various temperatures: initially at 20, 40 and 60 °C and then — at 35 °C.

To synthesize Co-NW, the basic solution of the following composition was used: $CoSO_4 \cdot 7H_2O$ — 320 g/l; H_3BO_3 — 40 g/l. The solution acidity varied and was controlled by a pH-meter. Two types of electrolytes were produced from the initial solution (with pH of around 4) by adding small quantities of acid or alkali. Thus, the solutions with high acidity (pH of around 3) were produced by adding sulfuric acid to the initial solution. The solutions with low acidity (pH of around 5) were produced by adding the ammonia solution. Use of these electrolytes made it possible to obtain two types of Co-NW samples. In all cases the process was carried out at the voltage of 0.9 V at 35 °C.

Note that the selection of the modes depended on the available data: thus, from the literature it is known that the cobalt structure may vary as the electrolyte pH changes, and from the electrochemistry manuals the strong dependence of nickel electric deposition on temperature is known.

Prior to irradiation and all studies (except for the preliminary X-ray diffraction one), a growth polymer matrix was removed from the obtained samples. The matrix is a dielectric, and its presence would have distorted the results of both the irradiation and the microscopic analysis. The matrix was removed by the standard method — by its dissolution in the concentrated solution of NaOH alkali at 50–60 °C. Then the samples, which after separation were an array of NWs fixed at the common growth base from copper (parallel to the surface of the growth matrix), were washed in distilled water and dried in air.

2.2. Irradiation

Ion beam treatment of the prepared NWs of three types was carried out by continuous ion beams Ar^+ on ILM-1 setup equipped with a technological ion source „PULSAR-1M“ based on the glow discharge of low pressure with a cold hollow cathode [43]. Ions Ar^+ were used with energy of $E = 15$ keV, the ion current density was $j = 100\,\mu$m/cm^2, the fluence of ions was $F = 8.6 \cdot 10^{11}$–$6.3 \cdot 10^{15}$ cm^{-2}. Some samples were irradiated, by moving above them the plate with a hole of a certain width (3 and 30 mm) with the speed of 30 mm/s. This made it possible to avoid the substantial heating of the samples in process of irradiation. Low fluences of ions $8.6 \cdot 10^{11}$ and $8.6 \cdot 10^{12}$ cm^{-2} were developed with the help of a linear gate (exposure diaphragm) with an electromagnetic drive in order to specify the low exposures (0.001–1 s) [44]. The NWs irradiation modes are given in the table.

The values of the average projective runs of ions Ar^+ in the studied materials calculated using Monte Carlo modelling method in SRIM software [45], are ~ 7.5 nm for ions with energy of 15 keV.

The structure and the magnetic properties were studied in the initial samples and samples after irradiation.

Modes of irradiation with ions of Ar^+ NW from nickel and cobalt: energy of ions E, current density of bundle j, width of diaphragm L, movement speed of target v, number of passes n, irradiation time t, fluence of ions F

Item No.	E, keV	j, μA/cm^{-2}	L, mm	v, mm/s	n	t, s	F, cm^{-2}
1	15	100	Using a linear gate with exposure of 0.00138 s		1	0.00138	$8.6 \cdot 10^{11}$
2					10	0.0138	$8.6 \cdot 10^{12}$
3			3	30	1	0.1	$6.3 \cdot 10^{13}$
4			30	30	1	1	$6.3 \cdot 10^{14}$
5			30	30	10	10	$6.3 \cdot 10^{15}$

2.3. Structural studies

The samples (initial and after irradiation) were studied by the X-ray and microscopic methods. The X-ray diffraction analysis was carried out on RIGAKU Miniflex diffractometer (CuK_α, $U = 40$ kV, $I = 15$ mA, angle interval 20–100°, pitch 0.2°). The studies with the scanning electron microscopy (SEM) were carried out using JEOL JSM 6000 plus (secondary electron mode, accelerating voltage of 15 kV; preliminary studies) and SCIOS (secondary electron mode, accelerating voltage 2 kV, current 10 nA; images with high resolution) instruments.

2.4. Magnetic measurements

Magnetic measurements were carried out using a magnetometer with a vibrating sample of LakeShore 7407 (USA) model in the fields of up to 16 kOe at room temperature. Hysteresis loops were measured at two mutually perpendicular orientations of the sample: in the plane and perpendicular to the plane of the copper substrate corresponding to the directions perpendicularly to the NW axes and along NW axes. The studied samples had the form of rectangles (with area of 9–11 mm^2), which were fixed on the measuring stem so that the direction of the magnetic field in one of the cases (field in the plane) matched the larger side of the sample. The produced hysteresis loops were used to determine the magnetization of saturation, residual magnetization and coercive force (CF).

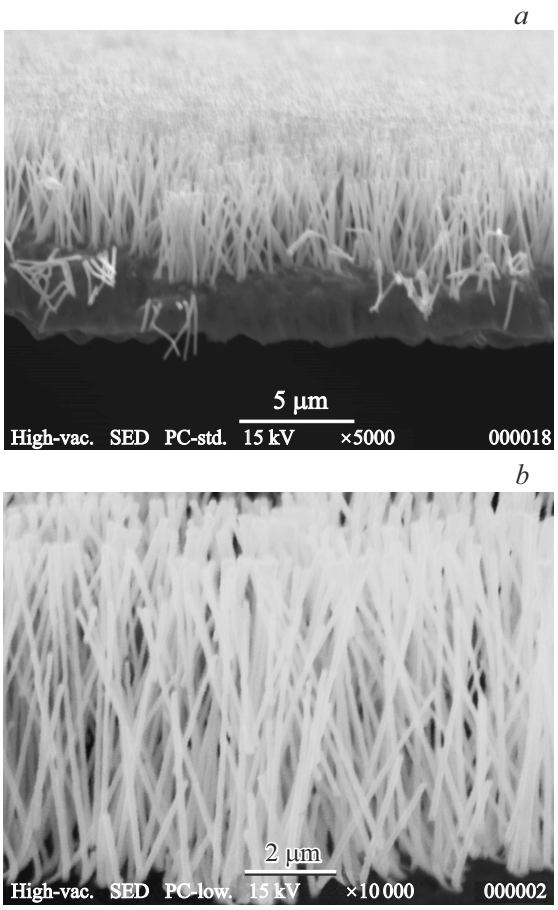

Figure 1. SEM-image of the obtained samples: *a*) Ni-NW, *b*) Co-NW (with a cubic lattice).

3. Results and discussion

Three types of nickel NWs (with different synthesis temperature) and two types of cobalt NWs (at different pH values of electrolyte) were obtained.

3.1. NWs array certification

Examples of SEM-images of the produced NWs arrays (after separation of the polymer matrix) are given in Figure 1.

The analysis of the images shows that the formed structures have the appearance of a multitude (array) of long threads — NWs. All NWs have the length of the order of 5–7 μm (which corresponds to the conditions of growth — in particular, the passed charge), and their diameter corresponds to the diameter of the pore channels of 100 nm.

X-ray diffraction studies were performed for all samples. Figure 2 shows the diffraction pattern of nickel samples, and Figure 3 — cobalt ones.

X-ray diffraction analysis showed that all samples with Ni-NWs have FCC structure. The increase of the growth temperature causes the reduction in the peak width,

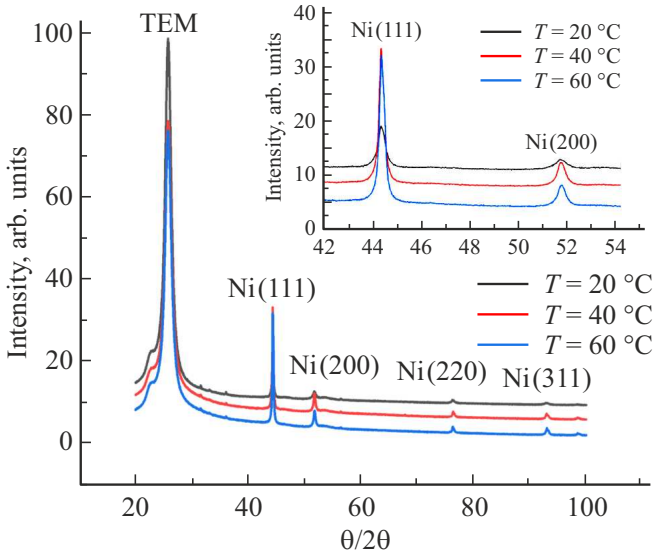

Figure 2. Diffraction pattern of NWs samples from Ni, obtained at temperatures of 20, 40 and 60 °C (indicated in the figure); nickel lines are indicated, TEM-peak of the matrix; on the insert — the diffraction pattern fragment.

which is most probably caused by the increase in the grain size. Co-NW structure depends on the synthesis conditions. Thus, the growth in electrolyte with pH ≈ 3 the NWs were formed with a cubic lattice, whereas the decrease in the acidity (pH ≈ 5) caused production of NWs with a hexagonal lattice. Note that the impact of the solution acidity at the growth of Co-NWs was observed previously as well — in [19,20] it is shown that the decrease in the electrolyte acidity causes a transition from the cubic structure to the hexagonal one. However, the described results were obtained for other matrices (PAO) and other deposition conditions.

The work was further carried out with the certified samples of several types — three types of samples with nickel NWs (with a cubic structure), produced at different temperature, and samples of cobalt NWs (with a cubic and hexagonal structure).

3.2. Magnetometry of initial samples

Figure 4 shows the obtained hysteresis loops for the nickel samples synthesized at different temperatures.

The observed differences of the hysteresis loops at two orientations of the magnetic field are related to the impact of the form anisotropy of both NWs as such and the samples, which were measured. Following the results of the completed measurements, the main magnetic parameters were estimated, the values of which are given in Figure 5.

Analysis of the hysteresis loops and table data makes it possible to conclude that the electric deposition temperature affects strongly the main magnetic parameters. Temperature increase from 20 to 60 °C causes tripling of saturation magnetization and doubling off coercive force. Taking into account the conclusion on the increase of the crystallite size (made on the basis of X-ray data), one may assume that the temperature increase causes noticeable increase in the growth speed and increase of the defectivity of these crystallites. Based on the obtained results, the sample for subsequent experiments (irradiation) was grown at 35 °C.

Two types of cobalt samples with different crystalline lattices found by X-ray method demonstrated noticeably different magnetic parameters (described below).

3.3. Ionic irradiation

The effect of irradiation on the magnetic properties of samples of Ni-NWs obtained at temperature 35 °C, and samples of Co-NWs in the cubic and hexagonal modification. Series of their irradiation with ions were carried out. The experimental conditions are described above. Fluences increased in series and were $8.6 \cdot 10^{11}$, $8.6 \cdot 10^{12}$, $6.3 \cdot 10^{13}$, $6.3 \cdot 10^{14}$ and $6.3 \cdot 10^{15}$ cm^{-2}. (In the subsequent discussion and on the curves only the order of magnitude of the fluences will be specified).

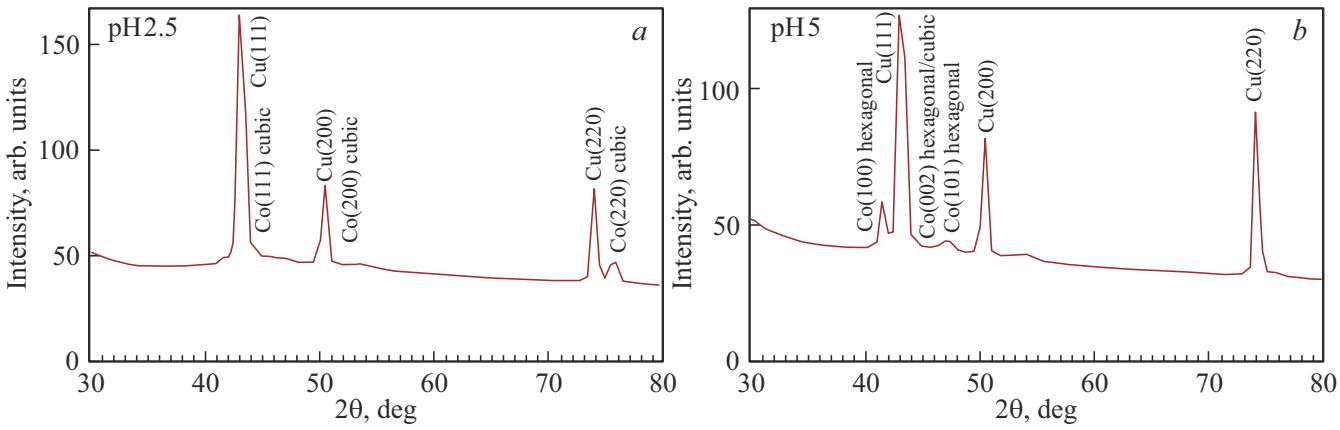

Figure 3. Diffraction pattern of NW samples from Co, obtained using electrolyte with *a*) pH = 3 and *b*) pH = 5; cobalt and copper lines are indicated.

3.4. Studies of the sample structure after irradiation

The obtained SEM-images of three types of NWs after irradiation with the maximum fluence are given in Figure 6.

The analysis of the produced images shows that Ni-NWs after the highest fluence of ions do not change their morphology — obviously this is related to their rather high radiation stability. And Co-NWs change significantly. Mostly the tips of NWs change— obviously other „in-depth“ parts of NWs are less exposed to the irradiation being screened by their neighbors. It may be noted that sometimes the formed structures have hexagonal shape.

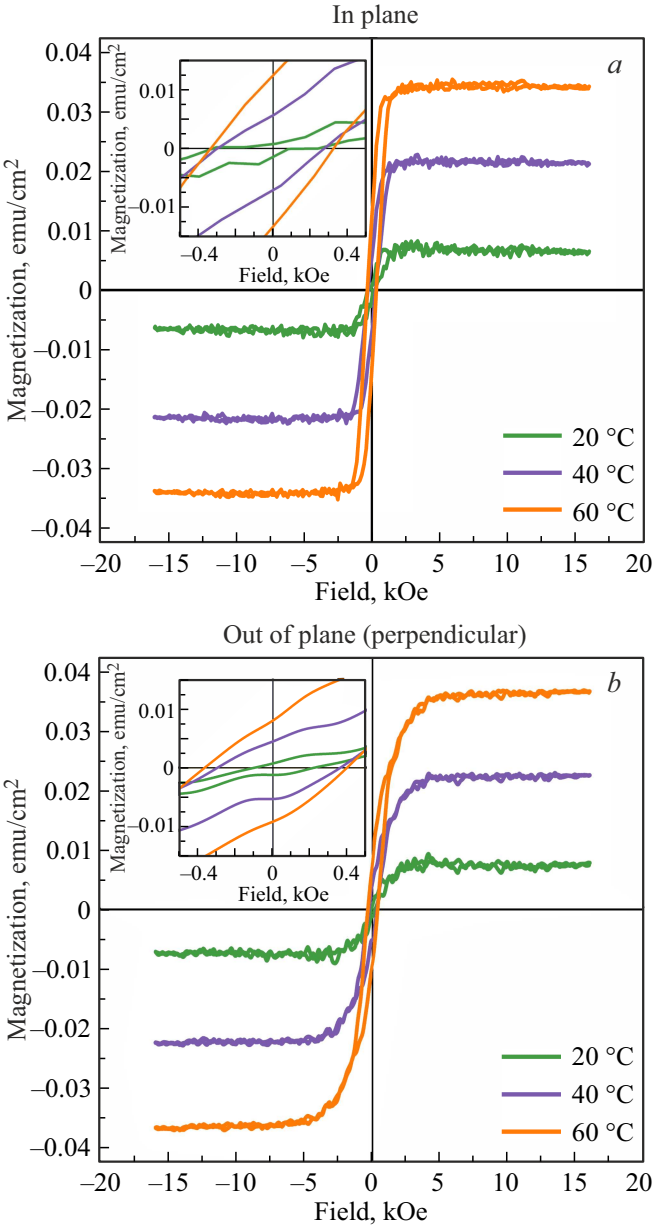

Figure 4. Hysteresis loops of samples of Ni-NWs obtained at different temperatures (indicated in the figure), at various orientations of the external magnetic field: *a*) in-plane, *b*) out-of-plane.

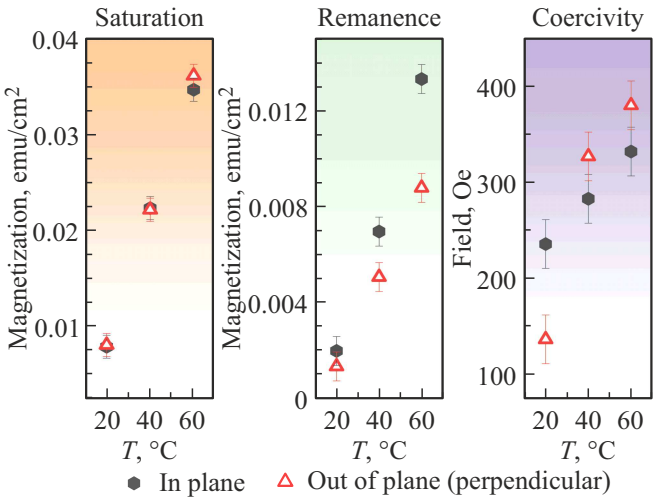

Figure 5. Dependences of saturation magnetization, residual magnetization and coercive force on temperature.

Theoretically — with account of the NW density and incidence angle of the irradiation ion bundle — you may approximately estimate the lengths of the distorted parts of NWs: from 0.7 to 1.5 μm. This amounts to approximately 10–20% of the initial length of NWs, and the volume change is same.

Note that the fusion temperature of cobalt is rather high (1495 °C); such temperature may not be achieved in the irradiation experiments (note that the fusion temperature of the volume nickel is rather high and is also not achieved when NWs are irradiated). The possible cause for the observed changes of Co-NWs may be recrystallization induced by irradiation. (Oxides may also be formed, however, this seems to be less probable). The significant difference between cobalt and nickel is the fact that heat conductivity of cobalt is nearly one point five times less than that of nickel; this factor may cause a much more significant heating of the tips of cobalt NWs upon irradiation.

It is known that the so called „radiation jiggle“ [46,47] with elastic and shock waves increases the migration mobility of the atoms. The diffusion constant may increase thousands of times. Previously papers [48,49] have shown that under ion irradiation the migration mobility of the atoms increases numerously, which causes the processes of recrystallization at lower temperatures, besides, for different materials the decrease in the recrystallization temperature will vary. (It was noted previously that the difference in the behavior of different materials is hard to predict even for the volume materials and more so for nanoobjects.) But then again the tips of NWs may oxidize: thus, the susceptibility to more intense oxidation in air was shown in [50], where it was demonstrated that oxides with hexagonal habitus are formed on the surface of cobalt-containing NWs. For more precise detection of the cause for the NW shape change, the composition of the produced structures and the effect

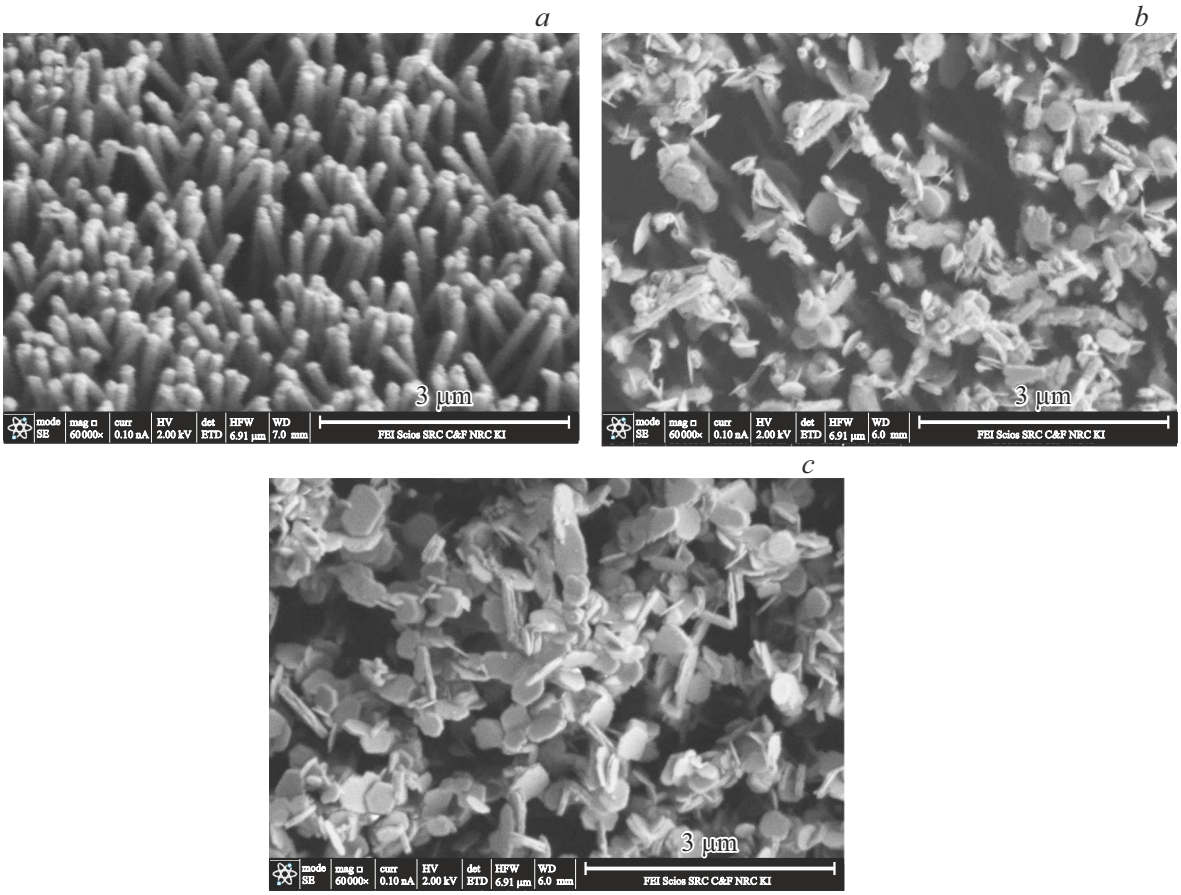

Figure 6. Microphotographs of samples after irradiation with maximum fluence: *a*) nickel samples, *b*) samples of NWs from cubic cobalt, *c*) samples of NWs from hexagonal cobalt.

depending on the fluence of ions, additional studies are planned.

It is important to note that the conducted X-ray diffraction studies of the same samples found no significant differences from the initial ones.

3.5. Magnetometry of irradiated samples

Hysteresis loops were measured for all series of samples. Figures 7 and 8 show the obtained curves (for two directions of the applied magnetic field).

For all types of samples (both initial and irradiated ones) the axis of light magnetization is directed along the NW axes, which is confirmed by a stronger inclination of the hysteresis loops for the out-of-plane orientation of the magnetic field. Besides, the coercivity in the in-plane direction is higher than in the out-of-plane direction. Such behavior differs from the behavior of certain extended objects (for example, a single rod) and may be explained both by the interaction of the NWs between each other and by the fact that the NWs in the array have a certain spread of the slopes (average distances between the NWs were 200−300 nm, and the inclination angle varied within the limits of up to $\pm 20^\circ$). It should be noted that in the papers above the magnetic measurements provided various correlation of the coercivity value and the direction of the light axis: in some papers the coercivity was higher in direction of NWs (for example, in [19]), in other papers the high CF was observed in the direction perpendicular to NWs [20].

3.6. Effect of ion irradiation

Comparison of the data obtained shows the difference between the samples. Irradiation of the Co-NWs samples with the cubic type of the lattice causes a non-monotonic change in the magnetization of saturation (growth, then drop) and coercive force (drop, then growth). For Ni-NWs (FCC) the irradiation causes no change in the saturation magnetization and residual magnetization, the coercive force increases in the direction of hard magnetization. Different behavior of nickel and cobalt under irradiation may be related to the difference in the parameters of the magnetocrystalline anisotropy; such difference in the responses to the external exposure was noted, for example, in papers [46,47].

The strongest changes are observed when hexagonal cobalt NWs are irradiated. At the same time, as the ion

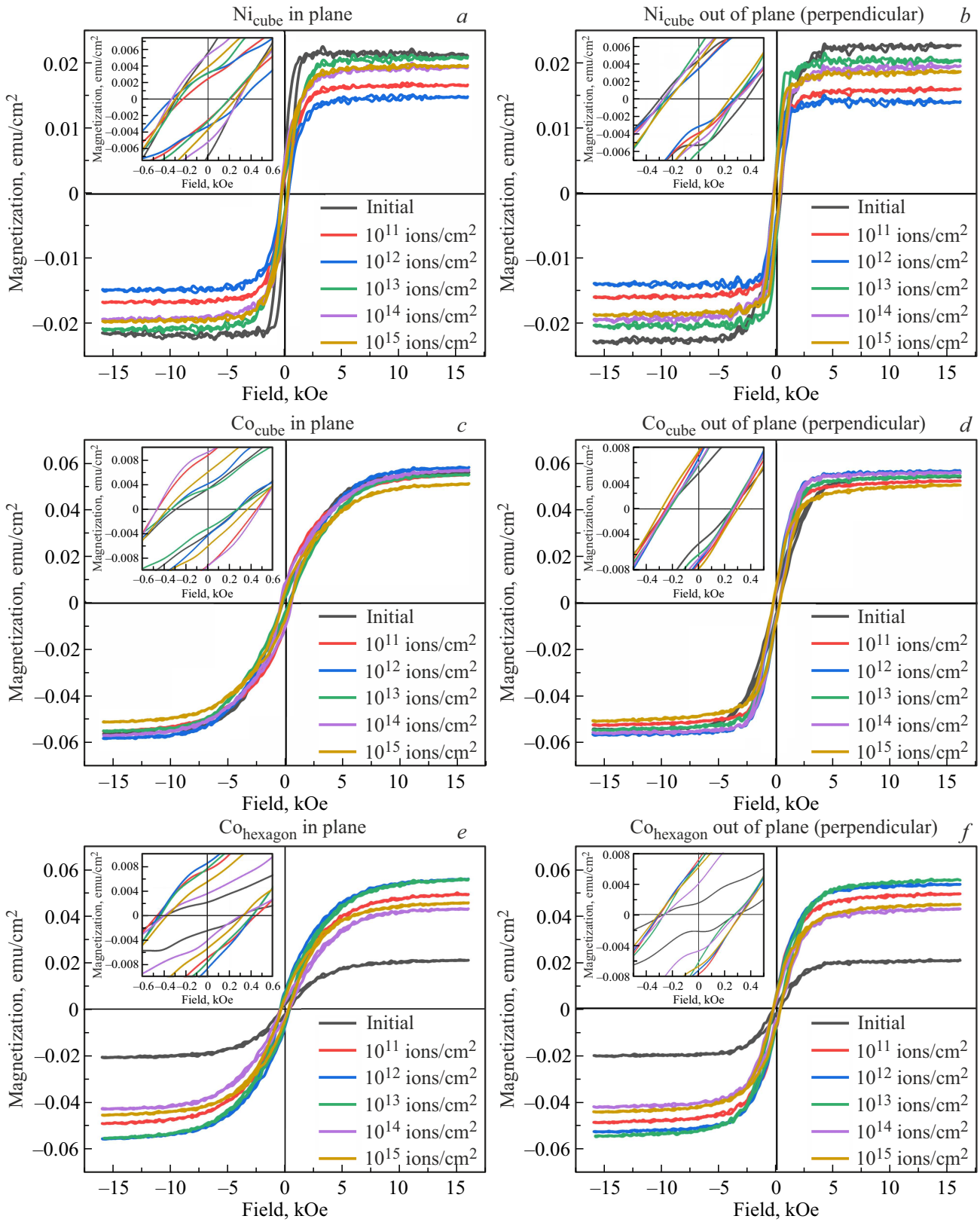

Figure 7. Magnetic parameters. Hysteresis loops after the three series of irradiated samples in two orientations relative to the external magnetic field: *a, c, e* — field in the sample plane; *b, d, f* — perpendicularly to the sample plane.

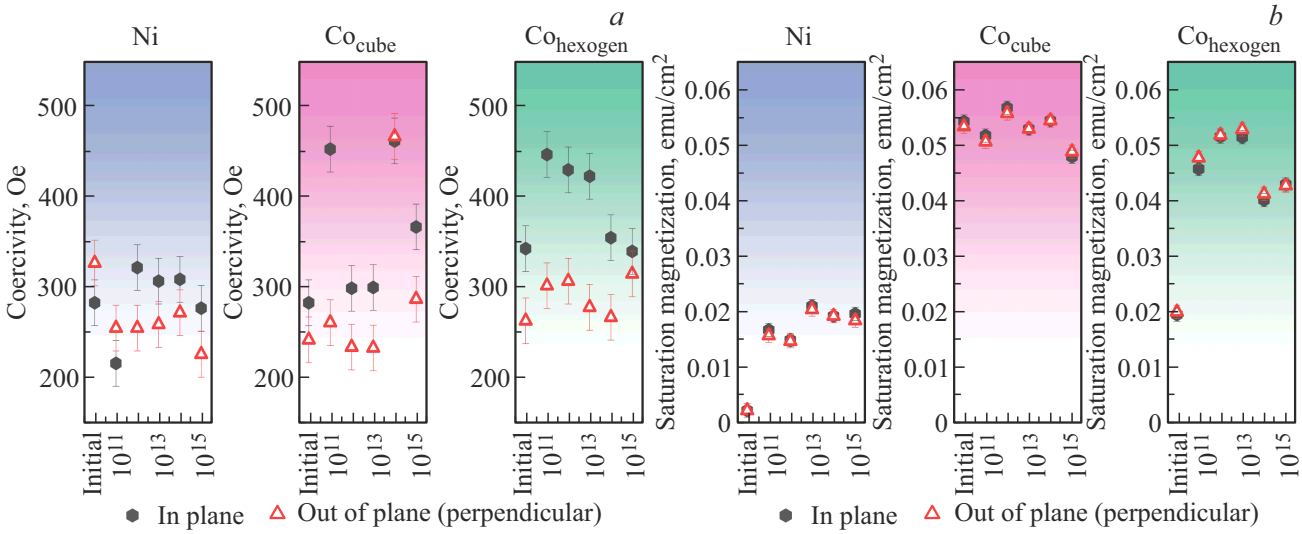

Figure 8. Summary data on all samples for *a*) coercivity and *b*) saturation magnetization. (The captions to the ion fluence values only contain the orders of magnitudes).

fluence increases, the magnetic parameters — saturation magnetization and CF — vary non-monotonically: first a significant growth, and then a minor drop is observed.

Non-monotonic nature of the changes may be explained by the presence of various mechanisms of studied materials exposure to the accelerated ions. This is formation of single Frenkel pairs, formation of the complexes of defects containing the introduced atoms, dense cascades of atomic displacements, and also annihilation of existing defects. It is possible that the competition (joint action) of these factors at the first stage causes the increase in the defectiveness of the structure, and then (when a certain boundary value is achieved) its relaxation (defect annihilation, their drainage in the grain boundaries or boundaries of NWs, etc.).

The cause for the complex dependences may be both irregularity of the effect at various parts of NWs: this is caused by mutual screening (presence of shadow areas) in the array of NWs. Besides, with the used energy the average projective run of argon ions is ~ 7 nm, which is considerably lower than the diameter of NWs (100 nm). As a result of this change in the various parts the NWs may be uneven, and the volume contribution of the irradiated parts of NWs into the change of the properties may amount to a minor share.

Since the X-ray tests found no significant structural changes upon irradiation, it may be stated that the magnetic measurements in this case are more sensitive to the radiation exposure. On the other hand, microscopy found noticeable changes in the morphology, but not of the whole NWs, but only their tips (which is obviously related to the highest effect of irradiation at the NW tips specifically). To determine what is happening in the ends of NWs — recrystallization or oxidation — additional experiments are required. Note that in this paper the microscopy assessed the local changes of only the NW parts, whereas the magnetometry and X-ray structure analysis provided an integral picture.

4. Conclusions

1. As the Ni-NW growth temperature increased from 20 to 60 °C their magnetization of saturation and coercive force increased three and two times (accordingly). The growth of Co-NW in electrolyte with pH ≈ 3 the structures were formed with a cubic lattice, whereas the decrease in the acidity (pH ≈ 5) caused production of NWs with a hexagonal lattice. Magnetization of saturation of NWs from cubic cobalt was approximately three times more than this characteristic in NWs from hexagonal cobalt, whereas the CF values were approximately same.

2. For all samples the similarity of the form of hysteresis loops for measurements in two geometries should be noted — „in-plane“ and „out-of-plane“ magnetic field, which indicates the relative isotropism of the samples.

3. For all samples the coercive force in „in-plane“ direction is higher than in „out-of-plane“ direction, which may be explained both by interaction of the adjacent NWs and their certain inclination in different directions.

4. Comparison of two modifications of Co-NW — cubic and hexagonal — showed that in the second case the effect of the ion irradiation is considerably stronger. This may be related to the smaller interplanar spacing in the HCP structure of cobalt.

5. Irradiation of NWs from hexagonal cobalt causes non-monotonic changes of their magnetic parameters: first the considerable growth of saturation magnetization and coercive force, and then a certain drop in these parameters is observed. Such dependence may be explained by the competition of various effects of ion irradiation. In Ni-NWs

and NWs from cubic cobalt it was not possible to detect the systematic connection of the changes to the ion fluence.

6. Ion irradiation changes strongly the topography of Co-NW tips. The shape of Ni-NWs will not change under similar exposure.

It may also be concluded that the change in the conditions of the growth conditions of NWs arrays and/or their subsequent irradiation with ions may be the effective methods to control their magnetic characteristics.

Acknowledgments

The authors would like to thank Yu.A. Alekhina (Faculty of Physics, Moscow State University) for the assistance in the measurement of magnetic parameters and V.V. Artemov (Research and Scientific Center Kurchatov Institute) for the precision SEM-studies.

Funding

R.A. Makarin would like to thank the „Basis“ foundation for the scholarship support. The synthesis of samples, their microscopy and X-ray tests were carried out using the equipment of the common use center „Structural Diagnostics of Materials“ of the Kurchatov Complex of Crystallography and Photonics of the Research and Engineering Center „Kurchatov Institute“, with the support of the Ministry of Science and Higher Education of the Russian Federation within the completion of the state assignment of the Research and Engineering Center „Kurchatov Institute“. The study and the analysis of the magnetic properties were performed under the State Assignment of the Lomonosov Moscow State University. Ion irradiation of samples and analysis of radiation changes were conducted within the state assignment of the Federal State Budget Scientific Institution Electrophysics Institute of Ural Branch of the Russian Academy of Sciences (subject No. 125020601676-4).

Conflict of interest

The authors declare that they have no conflict of interest.

References

[1] A.A. Eliseev, A.V. Lukashin. Funktsionalnye nanomaterialy. Fizmatlit, M. (2010). 456 s. (in Russian).
[2] V.M. Anischik, V.E. Borisenko, S.A. Zhdanok, N.K. Tolochko, V.M. Fedosyuk. Nanomaterialy i nanotekhnologii. Izd-vo BGU, Minsk (2008). 372 s. (in Russian).
[3] V.E. Borisenko, A.L. Danilyuk, D.B. Migas. Spintronika. Laboratoriya znanij, M. (2017). 229 s. (in Russian).
[4] H. Masuda, K. Fukuda. Sci. **268**, *5216*, 1466 (1995).
[5] C.R. Martin. Sci. **266**, *5193*, 1961 (1994).
[6] N. Lupu. Electrodeposited Nanowires and Their Applications. InTech, Croatia (2010). 236 p.
[7] M. Vazquez. Magnetic Nano- and Microwires: Design, Synthesis, Properties and Applications. Elsevier-Woodhead Publishing, Amsterdam (2015). 847 p.
[8] A.D. Davydov, V.M. Volgin. Russ. J. Electrochem. **52**, *9*, 806 (2016).
[9] S.V. Vonsovsky. Magnetizm. Nauka, M. (1984). 200 s. (in Russian).
[10] L.V. Kirensky. Magnetizm. Nauka, M. (1967), 196 s. (in Russian).
[11] D.J. Sellmyer, M. Zheng, R. Skomski. J. Phys.: Condens. Matter **13**, *25*, R433 (2001).
[12] H. Zeng, R. Skomski, L. Menon, Y. Liu, S. Bandyopadhyay, D.J. Sellmyer. Phys. Rev. B **65**, *13*, 134426 (2002).
[13] L. Piraux. Appl. Sci. **10**, *5*, 1832 (2020).
[14] T. Mehmood, A. Mukhtar, B. Shahzad Khan, K. Wu. Int. J. Electrochem. Sci. **1**, *8*, 6423 (2016).
[15] Yu.P. Ivanov, J. Leliaert, A. Crespo, M. Pancaldi, C. Tollan, J. Kosel, A. Chuvilin, P. Vavassori. ACS Appl. Mater. Interfaces **11**, *4*, 4678 (2019).
[16] J. Verbeeck, O.I. Lebedev, G. Van Tendeloo, L. Cagnon, C. Bougerol, G. Tourillon. J. Electrochem. Soc. **150**, *10*, E468 (2003).
[17] Y. Yang, Y. Chen, Y. Wu, X. Chen, M. Kong. J. Nanomater. **2010**, 793854 (2010).
[18] J. Duan, J. Liu, T.W. Cornelius, H. Yao, D. Moa, Y. Chen, L. Zhang, Y. Sun, M. Hou, C. Trautmann, R. Neumann. Nucl. Instr. Meth. Phys. Res. B **267**, *16*, 2567 (2009).
[19] F. Li, T. Wang, L. Ren, J. Sun. J. Phys.: Condens. Matter **16**, *45*, 8053 (2004).
[20] A. Lobo Guerrero, A. Encinas, E. Araujo, L. Piraux, J. de la Torre Medina. J. Phys. D: Appl. Phys. **56**, *6*, 065003 (2023).
[21] K. Nielsch, F. Müller, A.-P. Li, U. Gösele. Adv. Mater. **12**, *8*, 582 (2000).
[22] N. Adeela, K. Maaz, U. Khan, S. Karim, M. Ahmad, M. Iqbal, S. Riaz, X.F. Han, M. Maqbool. Ceram Int. **41**, *9 Part B*, 12081 (2015).
[23] D.C. Leitao, C.T. Sousa, J. Ventura, J.S. Amaral, F. Carpinteiro, K.R. Pirota, M. Vazquez, J.B. Sousa, J.P. Araujo. J. Non-Cryst. Solids **354**, *47–51*, 5241 (2008).
[24] Y.H. Chen, J.L. Duan, H.J. Yao, D. Mo, T.Q. Liu, T.S. Wang, M.D. Hou, Y.M. Sun, J. Liu. Physica B **441**, 1 (2014).
[25] V.V. Ovchinnikov. V kn.: Elektrofizika na Urale: chetvert veka issledovaniy / Pod red. V.G. Shpaka. UrBr RAN, Ekaterinburg (2011). Gl. 13. (in Russian).
[26] N.V. Gushchina, K.V. Shalomov, V.V. Ovchinnikov, N.S. Bannikova, M.A. Milyaev. Phys. Metals. Metallogr. **121**, *12*, 1168 (2020).
[27] N.V. Gushchina, F.F. Makhin'ko, V.V. Ovchinnikov, N.V. Kataeva, V.I. Voronin, V.I. Bobrovskii, V.V. Sagaradze. Phys. Metals. Metallogr. **122**, *3*, 307 (2021).
[28] G.G. Bondarenko. Radiatsionnaya fizika, struktura i prochnost tverdykh tel. Laboratoriya znanij, M. (2016). 463 s. (in Russian).
[29] R.A. Andrievski. Phys. — Uspekhi **57**, *10*, 945 (2014).
[30] S.K. Park, Y.K. Hong, Y.B. Lee, S.W. Bae, J. Joo. Curr. Appl. Phys. **9**, *4*, 847 (2009).
[31] H. Shehla, A. Ali, S. Zongo, I. Javed, A. Ishaq, H. Khizar, S. Naseem, M. Maaza. Chin. Phys. Lett. **32**, *9*, 096101 (015).
[32] S. Honey, S. Naseem, A. Ishaq, M. Maaza, M.T. Bhatti, D. Wan. Chin. Phys. B **25**, *4*, 045105-1 (2016).

[33] B. Bushra, H. Shehla, M. Madhuku, A. Ishaq, R. Khan, M. Arshad, A. Khalid, N. Shahzad, M. Maaza. Curr. Appl. Phys. **15**, *5*, 642 (2015).
[34] S.A. Bedin, F.F. Makhin'ko, V.V. Ovchinnikov, N.N. Gerasimenko, D.L. Zagorskiy. IOP Conf. Ser.: Mater. Sci. Eng. **18**, *1*, 012096 (2017).
[35] S.A. Bedin, V.V. Ovchinnikov, G.E. Remnev, F.F. Makhin'ko, S.K. Pavlov, N.V. Gushchina, D.L. Zagorskiy. Phys. Metals. Metallogr. **119**, *1*, 44 (2018).
[36] C. Chappert, H. Bernas, J. Ferré, V.V. Kottler, J.-P. Jamet, Y. Chen, E. Cambril, T. Devolder, F. Rousseaux, V.V. Mathet, H. Launois. Sci. **280**, *5371*, 1919 (1998).
[37] L.V. Chang, A. Nasruallah, P. Ruchhoeft, S. Khizroev, D. Litvinov. Nanotechnol. **23**, *27*, 275705 (2012).
[38] T. Devolder, J. Ferré, C. Chappert, H. Bernas, J.-P. Jamet, V. Mathet. Phys. Rev. B **64**, *6*, 064415 (2001).
[39] M.V. Sapozhnikov, N.S. Gusev, S.A. Gusev, D.A. Tatarskiy, Yu.V. Petrov, A.G. Temiryazev, A.A. Fraerman. Phys. Rev. B **103**, *5*, 054429 (2021).
[40] L. Herrera Diez, M. Voto, A. Casiraghi, M. Belmeguenai, Y. Roussigné, G. Durin, A. Lamperti, R. Mantovan, V. Sluka, V. Jeudy, Y.T. Liu, A. Stashkevich, S.M. Ch'erif, J. Langer, B. Ocker, L. Lopez-Diaz, D. Ravelosona. Phys. Rev. B **99**, *5*, 054431 (2019).
[41] I.L. Kalentyeva, O.V. Vikhrova, Yu.A. Danilov, A.V. Zdoroveyshchev, M.V. Dorokhin, Yu.A. Dudin, A.V. Kudrin, M.P. Temiryazeva, A.G. Temiryazev, S.A. Nikitov, A.V. Sadovnikov. Phys. Solid State **63**, *3*, 386 (2021).
[42] I.Yu. Pashenkin, R.V. Gorev, M.A. Kuznetsov, D.A. Tatarskiy, S.A. Churin, P.A. Yunin, M.N. Drozdov, D.O. Krivulin, M.V. Sapozhnikov, E.S. Demidov, V.A. Skuratov, E.V. Kudyukov, G.V. Kurlyandskaya, A.A. Fraerman, N.I. Polushkin. J. Phys. Chem. C **128**, *21*, 8853 (2024).
[43] N.V. Gavrilov, G.A. Mesyats, S.P. Nikulin, G.V. Radkovskii, A. Eklind, A.J. Perry, J.R. Treglio. J. Vac. Sci. Technol. A 999 **14**, *3*, 1050 (1996).
[44] K.V. Shalomov, V.V. Ovchinnikov, S.O. Cholakh. Diafragma ionnogo puchka: patent RF № RU189632U**1**. Byull. № 16 (2019). 6 s. (in Russian).
[45] SRIM−2013 The Stopping and Range of Ions in Matter. Available online: http://www.srim.org/SRIM/SRIM2011.htm (accessed on 29.10.2021).
[46] V.V. Ovchinnikov. Phys. — Uspekhi **51**, *9*, 955 (2008).
[47] V.V. Ovchinnikov. Surf. Coat. Technol. **35**, 65 (2018).
[48] N.V. Gushchina, V.V. Ovchinnikov, F.F. Makhin'ko, S.A. Linnik. J. Phys.: Conf. Ser. **830**, *1*, 012089 (2017).
[49] V.V. Ovchinnikov, N.V. Gushchina, S.M. Mozharovsky. Russ. Phys. J. **65**, *10*, 1657 (2023).
[50] O.M. Zhigalina, D.N. Khmelenin, I.M. Ivanov, I.M. Doludenko, D.L. Zagorskiy. Cristallogr. Reps **66**, *6*, 1109 (2021).

Translated by M.Verenikina